



Thermo-hydraulic rating of a shell and tube heat exchanger for methanol condensation

Evaluación térmico-hidráulica de un intercambiador de calor de tubo y coraza para la condensación de metanol

Amaury Pérez Sánchez ^{1,*}, Elizabeth Ranero González ¹, Eddy Javier Pérez Sánchez ²

¹ Universidad de Camagüey “Ignacio Agramonte Loynaz”, Facultad de Ciencias Aplicadas, Departamento de Ingeniería Química, Camagüey, Cuba.

² Empresa Servicios Automotores S.A., Dirección Comercial, Ciego de Ávila, Cuba.

*amauryes@nauta.es

(recibido/received: 04-mayo-2022; aceptado/accepted: 11-agosto-2022)

ABSTRACT

Shell and tube heat exchangers are the most common type of heat exchangers, and are applicable for a wide range of operating temperatures and pressures. In the present work the thermo-hydraulic rating of a shell and tube heat exchanger was carried out, in order to perform the condensation of a methanol stream using water as coolant. The overall heat transfer coefficient for both the sensible-heat and latent-heat zone had values of 166.41 W/m².K and 1,198.39 W/m².K, respectively; while the required total heat transfer area and percent excess area had values of 38.08 m² and 3.05 %, respectively. The pressure drops of methanol and water streams reached the values of 51,490.84 Pa and 2,890.50 Pa, respectively. The proposed shell and tube heat exchanger can be employed satisfactorily for the demanded heat transfer service, since the calculated percent excess area does not exceed 25%, and the pressure drop of the water stream does not exceed the value of 80,000 Pa.

Keywords: Methanol; Percent excess area; Pressure drop; Rating; Shell and tube heat exchanger.

RESUMEN

Los intercambiadores de calor de tubo y coraza son el tipo más común de intercambiadores de calor, y son aplicables para un amplio rango de temperaturas y presiones de operación. En el presente trabajo se efectuó la evaluación térmico-hidráulica de un intercambiador de calor de tubo y coraza, con el fin de efectuar la condensación de una corriente de metanol usando agua como agente de enfriamiento. El coeficiente global de transferencia de calor para tanto la zona de calor sensible como la de calor latente tuvo valores de 166,41 W/m².K y 1198,39 W/m².K, respectivamente; mientras que el área de transferencia de calor total requerida y el área porcentual en exceso tuvieron valores de 38,08 m² y 3,05%, respectivamente. Las caídas de presión de las corrientes de metanol y agua alcanzaron valores de 51 490,84 Pa y 2 890,50 Pa, respectivamente. El intercambiador de calor de tubo y coraza propuesto puede ser empleado satisfactoriamente para el servicio de transferencia de calor demandado, debido a que el área porcentual en exceso no excede el 25%, y la caída de presión de la corriente de agua no excede el valor de 80 000 Pa.

Palabras claves: Metanol; Área porcentual en exceso; Caída de presión; Evaluación; Intercambiador de calor de tubo y coraza.

NOMENCLATURE

a_s	Shell-side flow area	m^2
a_t	Tube-side flow area	m^2
A	Heat transfer area	m^2
A_{cond}	Condenser heat transfer area	m^2
$\% A_{exc}$	Percent excess area	$\%$
B	Baffle spacing	m
c	Clearance between tubes	m
C_p	Specific heat	$J/kg.K$
d_e	External diameter of the tubes	m
d_i	Internal diameter of the tubes	m
D_{eq}	Shell equivalent diameter	m
D_s	Shell diameter	m
f	Friction factor	-
f_s	Friction factor of the shell-side fluid	-
F_t	LMTD correction factor	-
G	Mass velocity	$kg/m^2.s$
G''	Flow per unit length on a horizontal condensate layer	$kg/m.s$
h	Film heat transfer coefficient	$W/m^2.K$
h_f	Film heat transfer coefficient of the shell-side fluid for the condensation of a vapor on a film without considering the effect of vapor velocity	$W/m^2.K$
h_i	Internal film heat transfer coefficient for the tube-side fluid	$W/m^2.K$
h_{io}	Internal film heat transfer coefficient for the tube-side fluid referred to the external area	$W/m^2.K$
$h_{h\lambda}$	Film heat transfer coefficient of the shell-side fluid in the latent-heat zone corrected by vapor velocity	$W/m^2.K$
H	Parameter	-
k	Thermal conductivity	$W/m.K$
LMTD	Logarithmic Mean Temperature Difference	$^{\circ}C$
L_t	Tube length	m
m	Mass flowrate	kg/s
\bar{m}_h	Average mass flowrate of the hot fluid	kg/s
n	Number of tube passes	-
N	Number of tubes	-
N_B	Number of baffles	-
N_s	Number of shell passes	-
Nu_f	Nusselt number of the shell-side fluid in the latent-heat zone without considering the influence of the vapor velocity	-
Nu_{λ}	Nusselt number of the shell-side fluid in the in the latent-heat zone corrected for the vapor velocity	-
P	Pressure	Pa
P	Coefficient	-

Pr	Prandtl number	-
P_t	Tube pitch	m
P_x	Parameter for F_t calculation	-
Δp_r	Pressure drop in return headers	Pa
Δp_s	Pressure drop of the shell-side fluid for the inlet mass flow	Pa
Δp_t	Pressure drop along the tubes	Pa
Δp_T	Total pressure drop of the tube-side fluid	Pa
ΔP	Allowable pressure drop	Pa
Q	Heat exchanged	W
R	Fouling factor	$K.m^2/W$
R	Coefficient for F_t calculation	-
Re	Reynolds number	-
S	Coefficient for F_t calculation	-
t	Temperature of the cold fluid	$^{\circ}C$
\bar{t}	Mean temperature of the cold fluid	$^{\circ}C$
\bar{t}_λ	Average temperature of the cold fluid in the condensation zone	$^{\circ}C$
t_3	Temperature of the cold fluid at the fictitious transition point	$^{\circ}C$
T	Temperature of the hot fluid	$^{\circ}C$
T_{sat}	Saturation (condensing) temperature of the hot fluid	$^{\circ}C$
T_w	Tube wall temperature	$^{\circ}C$
ΔT	Effective mean temperature difference	$^{\circ}C$
U	Overall heat transfer coefficient	$W/m^2.K$
v	Velocity	m/s
X	Parameter	-

Greek symbols

α	Coefficient	
ρ	Density	kg/m^3
μ	Viscosity	Pa.s
λ	Heat of condensation	J/kg

Subscripts

1	Inlet
2	Outlet
c	Cold fluid
h	Hot fluid
L	liquid
s	Desuperheating or sensible-heat zone
T	Total
v	Vapor
w	At the tube wall temperature
λ	Condensing or latent-heat zone

1. INTRODUCTION

In most industrial fields, cooling and heating fluids are needed. The device utilized to implement the heat transfer between the fluids is termed as heat exchanger (Yousufuddin, 2018).

Heat exchanger is a universal device in many industrial applications and energy conversion systems (Rao and Raju, 2016). A heat exchanger is an apparatus or equipment built for efficient heat transfer between two or more fluid streams at different temperatures (Nigusse *et al.*, 2014). Usually, heat exchangers remove the heat of a particular medium by allowing it to absorb into another heat transfer medium such as water, oil, air, etc. Currently, numerous heat exchanging techniques are available and are widely used in the applications such as refrigeration, air conditioning, automobiles, process industry, solar water heater systems, thermal power plants, and so forth (Abeykoon, 2014).

Various heat exchangers for industrial processes and systems have been designed. Among them, the shell-and-tube heat exchanger is the most common type (Arani *et al.*, 2016).

Shell-and-tube heat exchangers (STHXs) are widely used in many industrial areas, and more than 35–40% of heat exchangers are of this type due to their robust geometry construction, easy maintenance, and possible upgrades (Zhang *et al.*, 2010). According to (Abeykoon, 2014), STHXs are widely popular in petrochemical industry, power generation, energy conservation and manufacturing industry (Rao and Raju, 2016) due to their simplicity in design/manufacture, great sustainability to meet requirements, efficient thermal performance, structural simplicity, low costs, design flexibility and also the capability of adapting to different operating conditions.

In STHXs, one of the fluids flows inside the tubes while other fluid is forced through the shell and over the outside surfaces of the tubes (Fig. 1). Baffles are placed inside the shell to ensure a good circulation of the fluid within the shell across the tubes and hence they help to induce a high rate of heat transfer. Also, the heat transfer performance of the heat exchangers may reduce as they become older particularly due to fouling and scaling.

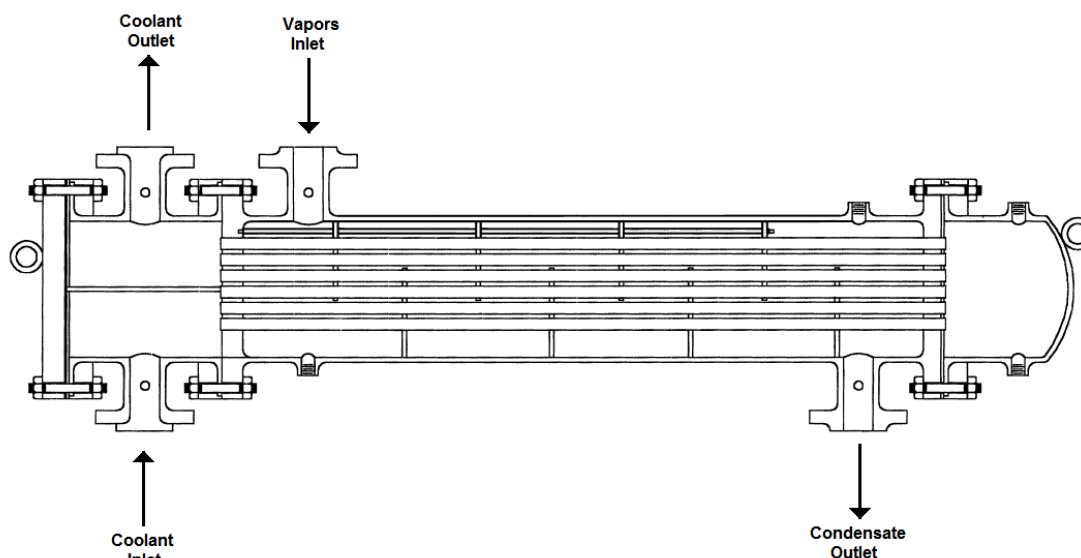


Figure 1. A two pass tube, baffled single pass shell, shell-and-tube heat exchanger.

Source: Adapted from (Kakaç *et al.*, 2012)

Two important problems in heat exchanger analysis are (1) rating existing heat exchangers and (2) sizing heat exchangers for a particular application. Rating involves the determination of the rate of heat transfer, the

change in temperature of the two fluids and the pressure drop across the heat exchanger (Ebierto & Eke, 2012), as well as the percent excess area (Cao, 2010).

Condensation heat transfer occurs in many engineering applications, such as in power condensers, boilers, and steam generators, which are all important components in conventional and nuclear power stations (Kakaç *et al.*, 2012).

Condensation is the process by which a vapor transforms into a liquid. For condensation to take place, it is necessary to remove heat from the condensing fluid by means of a cooling medium. If the vapor is a pure substance, as long as the pressure remains constant, condensation takes place isothermally. The temperature of the process is the saturation temperature of the vapor at the prevailing pressure. A condenser is a piece of equipment in which a vapor is condensed by heat extraction with a cooling medium (Cao, 2010).

A condenser is a two-phase flow heat exchanger in which heat is generated from the conversion of vapor into liquid (condensation) and the heat generated is removed from the system by a coolant. Condensers may be classified into two main types: those in which the coolant and condensate stream are separated by a solid surface, usually a tube wall, and those in which the coolant and condensing vapor are brought into direct contact. Condensers in which the streams are separated may be subdivided into three main types: air-cooled, shell-and-tube, and plate. In shell-and-tube condensers, the condensation may occur inside or outside the tubes. The orientation of the unit may be vertical or horizontal (Kakaç *et al.*, 2012). The most used cooling medium in condensers is water (Cao, 2010).

To date several authors have evaluated the performance of condensers. In this sense, (Botsch & Stephan, 1997) presented a model to describe the behaviour of an industrial scale shell-and-tube condenser. The model can be used under steady-state as well as under transient conditions, and is able to predict vapour and condensate flow rates, pressure drop and the temperatures of the vapour, condensate, wall and coolant. The results of several simulations were compared with experimental data to achieve a validation of the model. Similarly (Soltan *et al.*, 2004) studied the effect of baffle spacing on heat transfer area and pressure drop for shell side condensation in the most common types of segmentally baffled shell and tube condensers, (TEMA E and J types with conventional tube bundles). As a result of this research a set of correlation were presented to calculate the optimum baffle spacing for segmentally baffled shell and tube condensers. Likewise, (Hajabdollahi *et al.*, 2011) carried out the thermo-economic optimization of a shell and tube condenser, based on two new optimization methods, namely genetic and particle swarm (PS) algorithms. The procedure is selected to find the optimal total cost, including investment and operation cost of the condenser. Initial cost included condenser surface area and operational cost included pump output power to overcome the pressure loss. The design parameters considered were tube number, number of tube pass, inlet and outlet tube diameters, tube pitch ratio and tube arrangements (30, 45, 60 and 90°). In other study, (Pačíska *et al.*, 2013) performed the thermal-hydraulic simulation of an unconventional horizontal cross-flow shell-and-tube steam condenser using three commercial software packages, that is: Chemstations CHEMCAD, Aspen Shell & Tube Exchanger and HTRI Xchanger Suite, where the operating parameters at the inlet of the apparatus, thermophysical properties of streams, and the geometry of the apparatus were taken from the operator of the condenser. The results obtained were then compared to experimental data, while the observed differences between acquired data (heat duty and outlet temperature, pressure, and vapour mass fraction) and data from the operator were the principal markers of suitability of each individual software package. Also, (Singh and Sarkar, 2018) accomplished the energy, exergy and economic assessments of a shell and tube condenser of 580-MW nuclear power plant out using different water-based hybrid nanofluids. The effect of nanoparticle concentration on reductions of coolant requirement, pumping power and operating cost were also investigated. (Isah *et al.*, 2019) assessed the performance of a stripper/gas overhead shell and tube condenser operating under steady state conditions in two stages in an ammonia plant. Two different methods were employed in monitoring the heat exchanger fouling, namely dirt factor trend method and a statistical control technique where a Cumulative Sum (CuSum) chart is used to check the stability of the process. Data were obtained through steady state monitoring and direct measurements from the plant. The data were analyzed using various energy equations and a computer program to determine the overall heat transfer coefficient, heat duty, capacity ratio, corrected log-mean-temperature

difference, fouling factor, temperature range of both fluids and effectiveness. Finally, (Pattanayak *et al.*, 2019) developed the correlation for heat transfer coefficient, condenser pressure, cooling water flow rate and velocity towards assessment of thermal performance of a shell and tube steam condenser using the data of actual operating condition of a typical Indian coal fired power plant with nominal generation capacity of 210000 kW. The characteristics of various parameters affecting the thermal performance of the steam condenser are presented for different operating conditions. The analysis includes development of correlation for the heat transfer coefficient, system effectiveness, condenser heat load and cooling water flow rate through a simulation model. The relationship proposed can be used for thermal performance evaluation of a steam surface condenser in actual running condition with basic measured operating data like cooling water inlet temperature and flow rate. The correlations for condenser thermal performance provided in this study contain no constant coefficients and are function of inlet condition of condenser.

In the present study the thermo-hydraulic rating of a proposed shell and tube heat exchanger is carried out, in order to perform the condensation of a methanol stream using water as coolant. Several evaluation parameters are calculated, being the most important the percent excess area and the pressure drop of both fluid streams. The results obtained of these parameters are compared with the maximum allowable values established by the process, to determine if the proposed heat exchanger is feasible to use for this heat transfer service.

2. MATERIALS AND METHODS

2.1. Problem definition

It's desired to condense 5,800 kg/h of a gaseous methanol stream with a feed temperature and pressure of 95 °C and 134,000 Pa, respectively. A shell and tube heat exchanger is available with the following design parameters:

- Type: TEMA S.
- Number of tubes: 164.
- Tube length: 4 m.
- External diameter of tubes: 0.01905 m.
- Internal diameter of tubes: 0.0148 m.
- Tube array: Square.
- Tube pitch: 0.0254 m.
- Shell diameter: 0.43815 m.
- Number of tube passes: 2.
- Number of shell passes: 1.
- Baffle spacing: 0.45 m.
- Number of baffles: 8.

The cooling agent will be water at an inlet temperature of 2 °C, while the outlet temperature of this fluid must not exceed 15 °C due to energetic safety reasons. The fluids will flow at countercurrent configuration inside the equipment, circulating the water inside the tubes and the methanol through the shell, and the heat exchanger will be located horizontally. The pressure drop of the chilled water should not exceed the value of 80,000 Pa, while the calculated percent excess area must not exceed 25%. It's necessary to know, from the thermo-hydraulic viewpoint, if this proposed heat exchanger is feasible to use for the intended heat transfer service.

2.2. Calculation methodology

To carry out the thermo-hydraulic evaluation of the proposed shell and tube heat exchanger, several correlation and equations published in (Cao, 2010) (Flynn et al., 2019) were used, by means of which it was determined some important evaluation parameters such as the percent excess area of the suggested equipment and the pressure drop of chilled water. Each of the steps used to carry out the evaluation of the proposed heat exchanger are presented next.

Percent excess area:

Step 1. Definition of the main initial parameters for both streams:

Table 1 shows the main initial parameters that must be defined for both streams.

Table 1. Main initial parameters to be defined for both streams.

Parameter	Cold fluid	Hot fluid	Unit
Mass flowrate	m_c	m_h	kg/s
Inlet temperature	t_1	T_1	°C
Outlet temperature	t_2	T_2	°C
Inlet pressure	P_c	P_h	Pa
Fouling factor	R_c	R_h	$m^2.K/W$
Allowable pressure drop	ΔP_c	ΔP_h	Pa

Source: Own elaboration.

In this case, the outlet temperature of the hot fluid (condensate) will be equal to the saturation temperature under the working pressure of this stream (P_h), that is: $T_2 = T_{sat}$.

Step 2. Main initial parameters of the proposed shell and tube heat exchanger:

Table 2 displays the main initial parameters that must be known for the proposed shell and tube heat exchanger (condenser).

Table 2. Main initial parameters of the proposed condenser.

Parameter	Symbol	Unit
Number of tubes	N	-
Tube length	L_t	m
External diameter of the tubes	d_e	m
Internal diameter of the tubes	d_i	m
Tube array	\square/Δ	-
Tube pitch	P_t	m
Shell diameter	D_s	m
Number of tube passes	n	-
Number of shell passes	N_s	-
Baffle spacing	B	m
Number of baffles	N_B	-

Source: Own elaboration.

Step 3. Determination of the saturation (condensing) temperature (T_{sat}) of the hot stream at the working pressure P_h .

Step 4. Mean temperature of the cold fluid (\bar{t}):

$$\bar{t} = \frac{t_1 + t_2}{2} \quad (1)$$

Step 5. Physical properties of the hot fluid both in the vapor and liquid state at the saturation temperature (T_{sat}):

Table 3 presents the main physical properties that must be determined for the hot fluid both in the vapor and liquid states.

Table 3. Physical properties that must be determined for the hot fluid in both vapor and liquid states.

Physical property	Vapor	Liquid	Unit
Density	$\rho_{h(v)}$	$\rho_{h(L)}$	kg/m ³
Viscosity	$\mu_{h(v)}$	$\mu_{h(L)}$	Pa.s
Thermal conductivity	$k_{h(v)}$	$k_{h(L)}$	W/m.K
Specific heat	$Cp_{h(v)}$	$Cp_{h(L)}$	J/kg.K
Heat of condensation		λ_h	J/kg

Source: Own elaboration.

Step 6. Physical properties of the cold fluid at the mean temperature determined in Step 4.

Table 4 exposes the physical properties that must be estimated for the cold fluid at the mean temperature calculated in Step 4.

Table 4. Physical properties to be estimated for the cold fluid at the mean temperature.

Physical property	Value	Unit
Density	ρ_c	kg/m ³
Viscosity	μ_c	Pa.s
Specific heat	Cp_c	J/kg.K

Source: Own elaboration.

Step 7. Heat exchanged in the condensation zone (Q_λ):

$$Q_\lambda = m_h \cdot \lambda_h \quad (2)$$

Step 8. Heat exchanged in the sensible-heat zone (Q_S):

$$Q_S = m_h \cdot Cp_{h(v)} \cdot (T_1 - T_{sat}) \quad (3)$$

Step 9. Total heat exchanged or heat load (Q_T):

$$Q_T = Q_\lambda + Q_S \quad (4)$$

Step 10. Mass flowrate of the cold fluid (m_c):

$$m_c = \frac{Q_T}{Cp_c \cdot (t_2 - t_1)} \quad (5)$$

Step 11. Temperature of the cold fluid at the fictitious transition point (t_3):

$$t_3 = t_2 - \frac{Q_s}{m_c \cdot Cp_c} \quad (6)$$

Step 12. Logarithmic Mean Temperature Difference (LMTD):

- Desuperheating (sensible-heat) zone (LMTD_s):

$$LMTD_s = \frac{(T_2 - t_3) - (T_1 - t_2)}{\ln \frac{(T_2 - t_3)}{(T_1 - t_2)}} \quad (7)$$

- Condensing (latent-heat) zone (LMTD_λ):

$$LMTD_\lambda = \frac{(T_2 - t_3) - (T_2 - t_1)}{\ln \frac{(T_2 - t_3)}{(T_2 - t_1)}} \quad (8)$$

Step 13. Coefficient R:

$$R = \frac{(T_1 - T_2)}{(t_2 - t_1)} \quad (9)$$

Step 14. Coefficient S:

$$S = \frac{(t_2 - t_1)}{(T_1 - t_1)} \quad (10)$$

Step 15. Parameter P_x:

$$P_x = \frac{1 - \left(\frac{R \cdot S - 1}{S - 1} \right)^{1/Ns}}{R - \left(\frac{R \cdot S - 1}{S - 1} \right)^{1/Ns}} \quad (11)$$

Step 16. LMTD correction factor (F_t):

$$F_t = \frac{\sqrt{R^2 + 1}}{R - 1} \cdot \frac{\ln \left[\frac{(1 - P_x)}{(1 - R \cdot P_x)} \right]}{\ln \left[\frac{\left(\frac{2}{P_x} \right) - 1 - R + \sqrt{R^2 + 1}}{\left(\frac{2}{P_x} \right) - 1 - R - \sqrt{R^2 + 1}} \right]} \quad (12)$$

Step 17. Effective mean temperature difference:

- Desuperheating (sensible-heat) zone (ΔT_s):

$$\Delta T_s = LMTD_s \cdot F_t \quad (13)$$

- Condensing (latent-heat) zone (ΔT_λ):

$$\Delta T_\lambda = LMTD_\lambda \cdot F_t \quad (14)$$

Step 18. Tube-side flow area (a_t):

$$a_t = \frac{\pi \cdot d_i^2}{4} \cdot \frac{N}{n} \quad (15)$$

Step 19. Velocity of the tube-side fluid (v_c):

According to the problem definition (Section 2.1), the cold fluid (water) will flow inside the tubes, while the hot condensing fluid (methanol) will circulate through the shell, thus:

$$v_c = \frac{m_c}{\rho_c \cdot a_t} \quad (16)$$

Step 20. Internal film heat transfer coefficient for the tube-side fluid (h_i):

According to (Cao, 2010) the film heat transfer coefficient for water flowing inside tubes can be calculated using the following equation:

$$h_i = 1423 \cdot (1 + 0.0146 \cdot \bar{t}) \cdot \frac{v_c^{0.8}}{d_i^{0.2}} \quad (17)$$

Step 21. Internal film heat transfer coefficient for the tube-side fluid referred to the external area (h_{io}):

$$h_{io} = h_i \cdot \frac{d_i}{d_e} \quad (18)$$

Sensible-heat zone calculations

Step 22. Clearance between tubes (c):

$$c = P_t - d_e \quad (19)$$

Step 23. Shell-side flow area (a_s):

$$a_s = \frac{D_s \cdot c \cdot B}{P_t} \quad (20)$$

Step 24. Shell equivalent diameter (D_{eq}):

- For a square pattern of the tubes:

$$D_{eq} = \frac{4 \cdot \left(P_t^2 - \frac{\pi \cdot d_e^2}{4} \right)}{\pi \cdot d_e} \quad (21)$$

Step 25. Reynolds number of the shell-side fluid in the sensible-heat zone [Re_{hs}]:

$$\text{Re}_{hs} = \frac{D_{eq} \cdot m_h}{a_s \cdot \mu_{h(v)}} \quad (22)$$

Step 26. Prandtl number of the shell-side fluid in the sensible-heat zone [Pr_{hs}]:

$$\text{Pr}_{hs} = \frac{Cp_{h(v)} \cdot \mu_{h(v)}}{k_{h(v)}} \quad (23)$$

Step 27. Film heat transfer coefficient of the shell-side fluid in the sensible-heat zone [h_{hs}]:

$$h_{hs} = 0.36 \cdot \left(\frac{k_{h(v)}}{D_{eq}} \right) \cdot \text{Re}_{hs}^{0.55} \cdot \text{Pr}_{hs}^{0.33} \quad (24)$$

Step 28. Overall heat transfer coefficient for the sensible-heat zone (U_s):

$$U_s = \frac{1}{\frac{1}{h_{io}} + \frac{1}{h_{hs}} + R_c + R_h} \quad (25)$$

Step 29. Required heat transfer area for the sensible-heat zone (A_s):

$$A_s = \frac{Q_s}{U_s \cdot \Delta T_s} \quad (26)$$

Latent-heat zone calculations

Step 30. Average mass flowrate of the hot fluid (\bar{m}_h):

$$\bar{m}_h = \frac{m_h}{2} \quad (27)$$

Step 31. Mass velocity of the hot fluid (G_h):

$$G_h = \frac{\bar{m}_h}{a_s} \quad (28)$$

Step 32. Reynolds number of the shell-side fluid in the latent-heat zone [$\text{Re}_{h\lambda}$]:

$$\text{Re}_{h\lambda} = \frac{d_e \cdot G_h \cdot \rho_{h(L)}}{\rho_{h(V)} \cdot \mu_{h(L)}} \quad (29)$$

Step 33. Coefficient P:

$$P = \frac{\rho_{h(L)} \cdot \mu_{h(L)}}{\rho_{h(V)} \cdot \mu_{h(V)}} \quad (30)$$

Step 34. Liquid Prandtl number of the shell-side fluid in the latent-heat zone [$\text{Pr}_{h\lambda}$]:

$$\text{Pr}_{h\lambda} = \frac{Cp_{h(L)} \cdot \mu_{h(L)}}{k_{h(V)}} \quad (31)$$

Step 35. Assumption of the wall temperature (T_w).

Step 36. Parameter H:

$$H = \frac{Cp_{h(L)} \cdot (T_{sat} - T_w)}{\text{Pr}_{h\lambda} \cdot \lambda_h} \quad (32)$$

Step 37. Parameter X:

$$X = 0.9 \cdot \left(1 + \frac{1}{P \cdot H} \right)^{0.33} \quad (33)$$

Step 38. Flow per unit length on a horizontal condensate layer (G''):

$$G'' = \frac{m_h}{L_t \cdot N^{2/3}} \quad (34)$$

Step 39. Film heat transfer coefficient of the shell-side fluid for the condensation of a vapor on a film without considering the effect of vapor velocity (h_f):

$$h_f = \frac{1.5 \cdot \left(\frac{4 \cdot G''}{\mu_{h(L)}} \right)^{-0.33}}{\left(\frac{\mu_{h(L)}^2}{k_{h(L)}^3 \cdot \rho_{h(L)}^2 \cdot g} \right)^{0.33}} \quad (35)$$

Step 40. Nusselt number of the shell-side fluid in the latent-heat zone without considering the influence of the vapor velocity (Nu_f):

$$Nu_f = \frac{h_f \cdot d_e}{k_{h(L)}} \quad (36)$$

Step 41. Nusselt number of the shell-side fluid in the latent-heat zone corrected for the vapor velocity (Nu_λ):

$$Nu_\lambda = \left(X^4 \cdot Re_{h\lambda}^2 + Nu_f^4 \right)^{0.25} \quad (37)$$

Step 42. Film heat transfer coefficient of the shell-side fluid in the latent-heat zone corrected by vapor velocity [$h_{h\lambda}$]:

$$h_{h\lambda} = \frac{Nu_\lambda \cdot k_{h(L)}}{d_e} \quad (38)$$

Step 43. Overall heat transfer coefficient for the latent-heat zone (U_λ):

$$U_\lambda = \frac{1}{\frac{1}{h_{io}} + \frac{1}{h_{h\lambda}} + R_c + R_h} \quad (39)$$

Step 44. Average temperature of the cold fluid in the condensation zone (\bar{t}_λ):

$$\bar{t}_\lambda = \frac{t_1 + t_3}{2} \quad (40)$$

Step 45. Verification of the wall temperature (T_w):

$$T_w = T_{sat} - \frac{U_\lambda \cdot (T_{sat} - \bar{t}_\lambda)}{h_{h(l)}} \quad (41)$$

The calculated value of T_w is accepted if it is within the range of ± 1.0 °C with respect to the value assumed in step 35. In the case that this condition is not fulfilled, the T_w value calculated by the equation (41) is substituted in the equation (32), and the calculation is repeated until the previous requisite is achieved.

Step 46. Required heat transfer area for the latent-heat zone (A_λ):

$$A_\lambda = \frac{Q_\lambda}{U_\lambda \cdot \Delta T_\lambda} \quad (42)$$

Step 47. Total heat transfer area required by the heat exchange system (A_T):

$$A_T = A_\lambda + A_S \quad (43)$$

Step 48. Condenser heat transfer area (A_{cond}):

$$A_{cond} = \pi \cdot d_e \cdot L_t \cdot N \quad (44)$$

Step 49. Percent excess area ($\% A_{exc}$):

$$\% A_{exc} = \left(\frac{A_{cond}}{A_T} - 1 \right) \cdot 100 \quad (45)$$

2.2. Pressure drop:

Step 50. Mass velocity of the tube-side fluid (G_c):

$$G_c = \frac{m_c}{a_t} \quad (46)$$

Step 51. Reynolds number of the tube-side fluid (Re_c):

$$\text{Re}_c = \frac{d_i \cdot G_c}{\mu_c} \quad (47)$$

Step 52. Friction factor of the tube-side fluid (f_t):

- Laminar flow ($\text{Re} \leq 2,100$):

$$f_t = \frac{16}{\text{Re}_c} \quad (48)$$

- Turbulent region ($\text{Re} > 2,100$):

$$f_t = 1.2 \cdot \left[0.0014 + (0.125 \cdot \text{Re}_c^{-0.32}) \right] \quad (49)$$

Step 53. Pressure drop of the tube-side fluid along the tubes (Δp_t):

$$\Delta p_t = 4 \cdot f_t \cdot n \cdot \frac{L_t}{d_i} \cdot \frac{G_c^2}{2 \cdot \rho_c} \cdot \left(\frac{\mu_c}{\mu_{cw}} \right)^\alpha \quad (50)$$

Where α is -0.25 for laminar flow and -0.14 for turbulent flow.

Step 54. Pressure drop of the tube-side fluid corresponding to the change in direction at the exchanger heads in a multipass heat exchanger (Pressure drop in return headers) (Δp_r):

$$\Delta p_r = 4 \cdot n \cdot \frac{G_c^2}{2 \cdot \rho_c} \quad (51)$$

Step 55. Total pressure drop of the tube-side fluid (Δp_T):

$$\Delta p_T = \Delta p_t + \Delta p_r \quad (52)$$

Step 56. Friction factor of the hot fluid in the shell-side (f_s):

- For $\text{Re}_{hs} < 500$:

$$f_s = \exp \left\{ 5.1858 - 1.7645 \cdot \ln(\text{Re}_{hs}) + 0.13357 \cdot [\ln(\text{Re}_{hs})]^2 \right\} \quad (53)$$

- For $\text{Re}_{hs} \geq 500$:

$$f_s = 1.728 \cdot \text{Re}_{hs}^{-0.188} \quad (54)$$

Step 57. Pressure drop of the hot fluid in the shell-side for the inlet mass flow (Δp_s):

$$\Delta p_s = f_s \cdot \frac{(N_B + 1) \cdot D_s}{D_{eq}} \cdot \frac{G_h^2}{2 \cdot \rho_{h(v)}} \cdot \left(\frac{\mu_{h(v)w}}{\mu_{h(v)}} \right)^{0.14} \quad (55)$$

3. RESULTS AND DISCUSSION

The results obtained when evaluating the proposed shell and tube heat exchanger are presented hereafter, specifically with respect to the determination of the percent excess area and the pressure drop of both streams.

3.1. Percent excess area

Step 1. Definition of the main initial parameters for both streams:

Table 5 shows the available initial data defined of both streams.

Table 5. Main available initial parameters defined for both streams.

Parameter	Water	Methanol	Unit
Mass flowrate	-	1.61	kg/s
Inlet temperature	2	95	°C
Outlet temperature	15	-	°C
Inlet pressure	-	134,000	bar
Fouling factor [†]	0.0003	0.0002	m ² .K/W
Allowable pressure drop	80,000	-	Pa

[†]Taken from (Sinnott, 2005).
Source: Own elaboration.

Step 2. Main initial parameters of the proposed shell and tube heat exchanger:

Table 6 exposes the main initial design parameters of the proposed shell and tube heat exchanger:

Table 6. Main initial design parameters of the proposed condenser.

Parameter	Symbol	Value	Unit
Number of tubes	N	164	-
Tube length	L _t	4.0	m
External diameter of the tubes	d _e	0.01905	m
Internal diameter of the tubes	d _i	0.0148	m
Tube array	□	Square	-
Tube pitch	P _t	0.0254	m
Shell diameter	D _s	0.43815	m
Number of tube passes	n	2	-
Number of shell passes	N _s	1	-
Baffle spacing	B	0.45	m
Number of baffles	N _B	8	-

Source: Own elaboration.

Step 3. Determination of the saturation (condensing) temperature (T_{sat}) of methanol at the working pressure P_h :

As denoted by (Green & Southard, 2019), the saturation (condensing) temperature of methanol at the pressure of 134,000 is 72 °C, therefore $T_{\text{sat}} = T_2 = 72 \text{ °C}$.

Step 4. Mean temperature of water (\bar{t}):

$$\bar{t} = \frac{t_1 + t_2}{2} = \frac{2 + 15}{2} = 8.5 \text{ °C}$$

Step 5. Physical properties of methanol both in the vapor and liquid state at the saturation temperature (T_{sat}):

Table 7 presents the main physical properties for methanol both in the vapor and liquid states, as referred by (Green & Southard, 2019).

Table 7. Physical properties of methanol both in vapor and liquid states.

Physical property	Vapor	Liquid	Unit
Density	1.60	740.94	kg/m ³
Viscosity	0.00001126	0.000322	Pa.s
Thermal conductivity	0.01979	0.1868	W/m.K
Specific heat	4,570.25	2,890.46	J/kg.K
Heat of condensation	1,085,768.39		J/kg

Source: Own elaboration.

Step 6. Physical properties of chilled water at the mean temperature determined in Step 4.

According to (Green & Southard, 2019) the chilled water will have the physical property values presented in Table 8 at the mean temperature calculated in Step 4.

Table 8. Physical properties of chilled water at the mean temperature.

Physical property	Value	Unit
Density	999.966	kg/m ³
Viscosity	0.001518	Pa.s
Specific heat	4,205.04	J/kg.K

Source: Own elaboration.

Table 9 shows the results of the parameters determined in steps 7-21.

Table 9. Results of the parameters determined in steps 7-21.

Step	Parameter	Symbol	Value	Unit
7	Heat exchanged in the condensation zone	Q_λ	1,748,087.11	W
8	Heat exchanged in the sensible-heat zone	Q_s	169,236.36	W
9	Total heat exchanged	Q_T	1,917,323.47	W
10	Mass flowrate of water	m_c	35.07	kg/s
11	Temperature of water at the fictitious transition point	t_3	13.85	°C
12	LMTD (Desuperheating zone)	LMTD _s	68.49	°C
	LMTD (Condensing zone)	LMTD _λ	64.05	°C

13	Coefficient R	R	1.769	-
14	Coefficient S	S	0.140	-
15	Parameter P_x	P_x	0.140	-
16	LMTD correction factor	F_t	0.993	-
17	Effective mean temperature difference (Desuperheating zone)	ΔT_s	68.01	°C
18	Effective mean temperature difference (Condensing zone)	ΔT_λ	63.06	°C
19	Tube-side flow area	a_t	0.0140	m ²
20	Velocity of water	v_c	2.51	m/s
21	Internal film heat transfer coefficient for water	h_i	7,756.51	W/m ² .K
22	Internal film heat transfer coefficient for water referred to the external area	h_{io}	6,026.05	W/m ² .K

Source: Own elaboration.

Figure 2 displays the temperature diagram of the condensing process, where the extreme and intermediate temperatures for each fluid stream are shown.

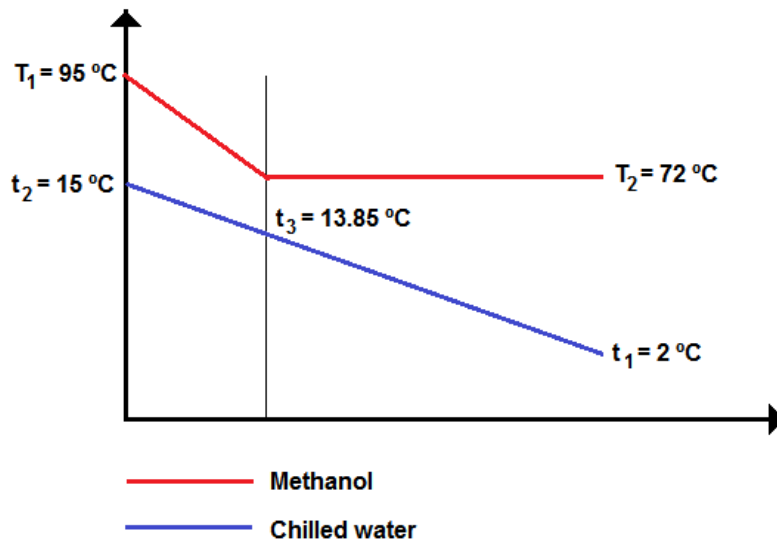


Figure 2. Temperature diagram of both fluid streams during the condensing process.

Source: Own elaboration.

Table 10 describes the results obtained of the steps 22-29, corresponding to the sensible-heat zone.

Table 10. Results of the parameters determined in steps 22-29.

Step	Parameter	Symbol	Value	Unit
22	Clearance between tubes	c	0.00635	m
23	Shell-side flow area	a_s	0.0493	m ²
24	Shell equivalent diameter	D_{eq}	0.0241	m
25	Reynolds number of methanol in the sensible-heat zone	Re_{hs}	69,909.91	-
26	Prandtl number of methanol in the sensible-heat zone	Pr_{hs}	2.60	-
27	Film heat transfer coefficient of methanol in the sensible-heat zone	h_{hs}	187.15	W/m ² .K

28	Overall heat transfer coefficient for the sensible-heat zone	U_s	166.41	W/m ² .K
29	Required heat transfer area for the sensible-heat zone	A_s	14.95	m ²

Source: Own elaboration.

Table 11 displays the results obtained of the parameters include in steps 30-34, corresponding to the latent heat zone.

Table 11. Results of the parameters determined in steps 30-34.

Step	Parameter	Symbol	Value	Unit
30	Average mass flowrate of methanol	\bar{m}_h	0.805	kg/s
31	Mass velocity of methanol	G_h	16.33	kg/m.s
32	Reynolds number of methanol in the latent-heat zone	$Re_{h\lambda}$	447,392.14	-
33	Coefficient P	P	13,242.82	-
34	Liquid Prandtl number of methanol in the latent-heat zone	$Pr_{h\lambda}$	4.98	-

Source: Own elaboration.

Step 35. Assumption of the wall temperature (T_w):

It's assumed a wall temperature of 60°C, which will be checked later in Step 45.

Table 12 indicates the results of the parameters calculated in steps 36-44.

Table 12. Results of the parameters calculated in steps 36-44.

Step	Parameter	Symbol	Value	Unit
36	Parameter H	H	0.0064	-
37	Parameter X	X	0.903	-
38	Flow per unit length on a horizontal condensate layer	G''	0.0134	kg/m.s
39	Film heat transfer coefficient of methanol for the condensation of a vapor on a film without considering the effect of vapor velocity	h_f	1,766.58	W/m ² .K
40	Nusselt number of methanol in the latent-heat zone without considering the influence of the vapor velocity	Nu_f	180.16	-
41	Nusselt number of methanol in the in the latent-heat zone corrected for the vapor velocity	Nu_λ	605.21	-
42	Film heat transfer coefficient of methanol in the latent-heat corrected by vapor velocity	$h_{h\lambda}$	5,934.55	W/m ² .K
43	Overall heat transfer coefficient for the latent-heat zone	U_λ	1,198.39	W/m ² .K
44	Average temperature of water in the condensation zone	\bar{t}_λ	7.925	°C

Source: Own elaboration.

Step 45. Verification of the wall temperature (T_w):

$$T_w = T_{sat} - \frac{U_\lambda \cdot (T_{sat} - \bar{t}_\lambda)}{h_{h(l)}} = 72 - \frac{1,198.39 \cdot (72 - 7.925)}{5,934.55} = 59.06 \text{ } ^\circ\text{C}$$

Since the calculated value of T_w is within the range of ± 1.0 °C with respect to the assumed value of T_w in step 35 (60 °C), there is no need of correct this value and repeat the calculation procedure.

Step 46. Required heat transfer area for the latent-heat zone (A_λ):

$$A_\lambda = \frac{Q_\lambda}{U_\lambda \cdot \Delta T_\lambda} = \frac{1,748,087.11}{1,198.39 \cdot 63.06} = 23.13 \text{ m}^2$$

Step 47. Total heat transfer area required by the heat exchange system (A_T):

$$A_T = A_\lambda + A_S = 14.95 + 23.13 = 38.08 \text{ m}^2$$

Step 48. Condenser heat transfer area (A_{cond}):

$$A_{cond} = \pi \cdot d_e \cdot L_t \cdot N = 3.14 \cdot 0.01905 \cdot 4 \cdot 164 = 39.24 \text{ m}^2$$

Step 49. Percent excess area ($\% A_{exc}$):

$$\% A_{exc} = \left(\frac{A_{cond}}{A_T} - 1 \right) \cdot 100 = \left(\frac{39.24}{38.08} - 1 \right) \cdot 100 = 3.05 \%$$

3.2. Pressure drop:

Table 13 exposes the results of the parameters considered in steps 50-57, corresponding to the pressure drop of both fluids.

Table 13. Results of the parameters considered in steps 50-57.

Step	Parameter	Symbol	Value	Unit
50	Mass velocity of water	G_c	2,505.0	kg/m ² .s
51	Reynolds number of water	Re_c	24,422.92	-
52	Friction factor of water (turbulent region)	f_t	0.00759	-
53	Pressure drop of water along the tubes [§]	Δp_t	51,490.84	Pa
54	Pressure drop in return headers	Δp_r	25,100.96	Pa
55	Total pressure drop of water	Δp_T	76,591.80	Pa
56	Friction factor of methanol in the shell-side	f_s	0.212	-
57	Pressure drop of methanol in the shell-side for the inlet mass flow [†]	Δp_s	2,890.50	Pa

Source: Own elaboration.

§ As suggested by (Cao, 2010) the factor $(\mu_c/\mu_{cw})^{0.14}$ is taken as 1.0.

† As recommended by (Cao, 2010) the factor $(\mu_{h(v)w}/\mu_{h(v)})^{0.14}$ is taken as 1.0.

Taking into account the results obtained in the calculation methodology, the heat exchanged in the condensation zone (Q_λ) is 10.3 times higher than the heat exchanged in the sensible heat zone (Q_S), which is

mainly due to the high value that presents the heat of condensation of methanol at the saturation temperature (1,085,768.39 J/kg).

Also, the internal film heat transfer coefficient for water referred to the external area had a value of 6,026.05 W/m².K, while the value of the film heat transfer coefficient of methanol in the latent-heat corrected by vapor velocity ($h_{h\lambda}$) is 31.7 times higher than the film heat transfer coefficient of methanol in the sensible-heat zone (h_{hs}). This is because the high value that presents the Reynolds number of methanol in the latent-heat zone, which increases the Nusselt number of methanol in the latent-heat zone corrected for the vapor velocity (Nu_{λ}), therefore increasing proportionally the value of $h_{h\lambda}$. It's worth to mention that the Reynolds number of methanol in the latent-heat zone (447,392.14) is 6.4 times superior to the Reynolds number of methanol in the sensible-heat zone (69,909.91).

Moreover, the overall heat transfer coefficient for the latent-heat zone (1,198.39 W/m².K) is 7.2 times higher than the overall heat transfer coefficient for the sensible-heat zone (166.41), which occurred basically because the high value of $h_{h\lambda}$ obtained.

Similarly, the calculated value for the required heat transfer area in the latent-heat zone (23.13 m²) is 1.54 times higher than the required heat transfer area for the sensible-heat zone (14.95 m²), which is due fundamentally to the elevated value obtained for the heat exchanged in the condensation zone.

It was obtained a calculated value of the percent excess area of 3.05%, which is lower than the maximum allowable limit established by the process (25%), while the pressure drop values of both the methanol and water streams were 2,890.50 Pa and 76,591.80 Pa, respectively. In this case, the calculated pressure drop of water is below the maximum allowable value set by the process (80,000 Pa).

Considering the results obtained, it could be concluded that the proposed shell and tube heat exchanger can be successfully used for the required condensing service, since the values of the percent excess area and the water pressure drop are within the limits established by the heat exchange system.

4. CONCLUSIONS

1. The thermo-hydraulic rating of a proposed shell and tube heat exchanger was performed in order to condense 5,800 kg/h of a gaseous methanol stream at an inlet temperature and pressure of 95 °C and 134,000 Pa respectively, by using chilled water as coolant at a feed temperature of 2 °C.
2. The total heat exchanged had a value of 1,917,323.47 W, while a chilled water mass flowrate of 35.07 kg/s will be necessary to carry out the condensation process.
3. The overall heat transfer coefficient for both the sensible-heat and latent-heat zones had values of 166.41 W/m².K and 1,198.39 W/m².K, respectively.
4. It was obtained a value of 38.08 m² for the required total heat transfer area.
5. The calculated percent excess area for the proposed equipment had a value of 3.05%, which is lower than the limit acceptable value established by the process (25%).
6. The calculated pressure drop for both the methanol and chilled water had values of 2,890.50 Pa and 51,490.84 Pa, respectively. In this case, the calculated pressure drop for chilled water didn't exceed the limit value established by the process (80,000 Pa).

7. The proposed shell and tube heat exchanger can be used for the required condensing process since the calculated percent excess area and the pressure drop of chilled water are below the maximum allowable values set by the heat exchange system.

REFERENCES

- Abeykoon, C. (2014). Improving the performance of shell-and-tube heat exchangers by the addition of swirl. *International Journal of Process Systems Engineering*, 2 (3), 221-245. doi:10.1504/IJPSE.2014.066691.
- Arani, A. A. A., Arefmanesh, A., and Uosofvand, H. (2016). Effect of baffle orientation on shell-and-tube heat exchanger performance. *Journal of Heat and Mass Transfer Research*, 4, 83-90. doi:10.22075/jhmtr.2017.1503.1100.
- Botsch, T. W., & Stephan, K. (1997). Modelling and simulation of the dynamic behaviour of a shell-and-tube condenser. *International Journal of Heat and Mass Transfer*, 40 (17), 4137-4149. doi:10.1016/S0017-9310(97)00019-7.
- Cao, E. (2010). *Heat transfer in process engineering*. New York, U.S.A.: McGraw-Hill.
- Ebieto, C. E., and Eke, G. B. (2012). Performance Analysis of Shell and Tube Heat Exchangers: A case study. *Journal of Emerging Trends in Engineering and Applied Sciences*, 3 (5), 899-903.
- Flynn, A. M., Akashige, T., and Theodore, L. (2019). *Kern's Process Heat Transfer (2nd ed.)*. Hoboken, U.S.A.: Scrivener Publishing.
- Green, D. W., and Southard, M. Z. (2019). *Perry's Chemical Engineers' Handbook (9th ed.)*. New York, U.S.A.: McGraw-Hill.
- Hajabdollahi, H., Ahmadi, P., and Dincer, I. (2011). Thermoeconomic optimization of a shell and tube condenser using both genetic algorithm and particle swarm. *International Journal of Refrigeration*, 34, 1066-1076. doi:10.1016/j.ijrefrig.2011.02.014.
- Isah, A., Sodiki, J. I., and Nkoi, B. (2019). Performance Assessment of Shell and Tube Heat Exchanger in an Ammonia Plant. *European Journal of Engineering Research and Science*, 4 (3), 37-44. doi:10.24018/ejers.2019.4.3.1145.
- Kakaç, S., Liu, H., and Pramuanjaroenkij, A. (2012). *Heat Exchangers: Selection, Rating and Thermal Design (3rd ed.)*. Boca Raton, U.S.A.: CRC Press.
- Nigusse, H. A., Ndiritu, H. M., and Kiplimo, R. (2014). Performance Analysis of a Shell Tube Condenser for a Model Organic Rankine Cycle for Use in Geothermal Power Plant. *International Journal of Engineering Research and Applications*, 4 (8), 141-147.
- Pačiska, T., Jegla, Z., Kilkovský, B., Reppich, M., and Turek, V. (2013). Thermal Analysis of Unconventional Process Condenser Using Conventional Software. *Chemical Engineering Transactions*, 35, 469-474. doi:10.3303/CET1335078.
- Pattanayak, L., Padhi, B. N., and Kodamasingh, B. (2019). Thermal performance assessment of steam surface condenser. *Case Studies in Thermal Engineering*, 14, 100484. doi:10.1016/j.csite.2019.100484.

Rao, J. B. B., and Raju, V. R. (2016). Numerical and heat transfer analysis of shell and tube heat exchanger with circular and elliptical tubes. *International Journal of Mechanical and Materials Engineering*, 11 (6), 1-18. doi:10.1186/s40712-016-0059-x.

Singh, S. K., and Sarkar, J. (2018). Energy, exergy and economic assessments of shell and tube condenser using hybrid nanofluid as coolant. *International Communications in Heat and Mass Transfer*, 98, 41-48. doi:10.1016/j.icheatmasstransfer.2018.08.005.

Sinnott, R. K. (2005). *Chemical Engineering Design* (4th ed. Vol. 6). Oxford, U.K.: Elsevier Butterworth-Heinemann.

Soltan, B. K., Saffar-Avval, M., and Damangir, E. (2004). Minimizing capital and operating costs of shell and tube condensers using optimum baffle spacing. *Applied Thermal Engineering*, 24, 2801–2810. doi:10.1016/j.applthermaleng.2004.04.005.

Yousufuddin, S. (2018). Heat Transfer Enhancement of a Shell and Tube Heat Exchanger with Different Baffle Spacing Arrangements. *Scholar Journal of Applied Sciences and Research*, 1 (6), 50-56.

Zhang, J.-F., He, Y.-L., and Tao, W.-Q. (2010). A Design and Rating Method for Shell-and-Tube Heat Exchangers With Helical Baffles. *Journal of Heat Transfer*, 132, 1-8.

SEMBLANCE OF THE AUTHORS



Amaury Pérez Sánchez: Obtained a degree in Chemical Engineering from the University of Camagüey, Cuba in 2009, where he is currently an instructor professor and assistant researcher. At the moment he is studying a Master in Biotechnology at the Center for Genetic Engineering and Biotechnology in Camagüey. He works in research lines related fundamentally with the design of heat and mass transfer equipment, simulation and optimization of processes and operations in the chemical industry using simulators such as SuperPro Designer® and ChemCAD®, and the techno-economic evaluation of processes and biotechnological plants.



Elizabeth Ranero González: Obtained a degree of Chemical Engineering from the University of Camagüey, Cuba in 2016. She works professionally as Instructor Professor at the University of Camagüey, Cuba. His research area includes the design and rating of heat and mass transfer equipment and processes, thermodynamic evaluation of chemical processes, and the simulation of biotechnological processes and systems.



Eddy Javier Pérez Sánchez: Obtained a degree in Chemical Engineering from the University of Camagüey, Cuba in 2016. He works professionally at Empresa de Servicios Automotores S.A., in the Department of Commercial Management. He works in research lines related with the design, rating and/or operation of heat and mass transfer equipment, as well as the simulation of petrochemical and biotechnological processes.